Single-Walled Carbon Nanotube/Phase Change Material Composites: Sunlight-Driven, Reversible, Form-Stable Phase Transitions for Solar Thermal Energy Storage

Yunming Wang, Bingtao Tang, and Shufen Zhang*

The development of solar energy conversion materials is critical to the growth of a sustainable energy infrastructure in the coming years. A novel hybrid material based on single-walled carbon nanotubes (SWNTs) and form-stable polymer phase change materials (PCMs) is reported. The obtained materials have UV-vis sunlight harvesting, light-thermal conversion, thermal energy storage, and form-stable effects. Judicious application of this efficient photo-thermal conversion to SWNTs has opened up a rich field of energy materials based on novel SWNT/PCM composits with enhanced performance in energy conversion and storage.

1. Introduction

Solar energy is the only renewable and carbon-neutral energy source of sufficient scale to replace fossil fuels.[1] Consequently, the research on and development of sustainable solar energy conversion and storage technologies have attracted a great deal of interest. Although the efficiency of energy conversion and storage devices depends on various factors, their overall performance strongly relies on the structure and property of the materials used.[1i,2] Various emerging nanomaterials have been studied for their efficient energy conversion and storage of solar irradiation.[3] Carbon nanomaterials, particularly single-walled carbon nanotubes (SWNTs),[4] are of particular interest as attractive candidates for energy applications because of their unique structure and properties[1f,5] for sunlight absorption and efficient solar energy conversion.

Photoinduced nanocarbons, operated as exothermic nanomaterials driven by sunlight, are one of the most attractive materials in modern chemistry.[4a,6] In the present study, a SWNT was successfully introduced to polyethylene glycol 10000 (PEG 10000)-co-*N*,*N*′-dihydroxyethyl aniline which was used as a form-stable polymer phase change material (PCM), thereby obtaining novel SWNT/PCM composites (**Figure 1**). The SWNTs were used as a nanoscale photon antenna that served as an effective photon capturer and molecular heater of the light-to-heat conversion process. Additionally, the SWNTs used to form the novel SWNT/PCM composites had a highly thermal conductivity,[7] by which the heat storage and release time of SWNT/PCM composites could be shortened. Therefore, our composites increased the energy utilisation efficiency during the heat charging and discharging processes. Compared with solar thermal water tanks with sensible heat storage (SHS) ($\eta < 0.6$),[2,8] the new SWNT/PCM composites have several smart features, such as latent heat storage (LHS) with high energy storage density, excellent flexibility, high light-to-heat and energy storage efficiency ($\eta > 0.84$). Simultaneously, the novel materials are able to harvest visible light and convert visible light to thermal energy effectively, as compared to the traditional organic phase change materials for latent heat thermal energy storage.[9] Thus, a rapid, visible sunlight-harvesting material, capable of light-thermal conversion and composed of a thermal storage material with a form-stable phase transition, was achieved. Upon solar irradiation, the SWNTs of the obtained SWNT/PCM composites perormed rapid and UV-vis sunlight-harvesting and light-thermal conversion. Simultaneously, the generated thermal energy was stored in the PCMs by a form-stable phase transition with a high energy storage density.[1i,10] Therefore, this novel sunlight-driven SWNT/PCM composites have important potential application in renewable and clean energy sources.

2. Results and Discussion

SWNTs are insoluble materials with a high aspect ratio, and they are strongly bundled to each other due to the strong inter-tube van der Waals interactions.[11] Thus, the dispersion of SWNTs in inorganic and organic solvents is quite difficult,[4b] which has hindered molecular level studies and device applications.[12] In this paper, we introduced nitrophenyl groups onto the SWNT surfaces by treating them with 4-nitrophenyldiazonium cations to obtain a uniform dispersion of SWNTs in a toluene system. The reason for this was that strong van der Waals forces existed between the nitrophenyl group of the surface-modified SWNTs and toluene. The encapsulating process of SWNTs by PCMs is shown in **Scheme 1** (see the Experimental Section for details). The form-stable PCMs were synthesized in toluene, and the resulting surface-modified SWNTs were then added and suspended in this solution by ultrasonication.[13]

Dr. Y. Wang, Dr. B. Tang, Prof. S. Zhang
State Key Laboratory of Fine Chemicals
Dalian University of Technology
Dalian 116024, P. R. China
E-mail: tangbt@dlut.edu.cn

DOI: 10.1002/adfm.201203728

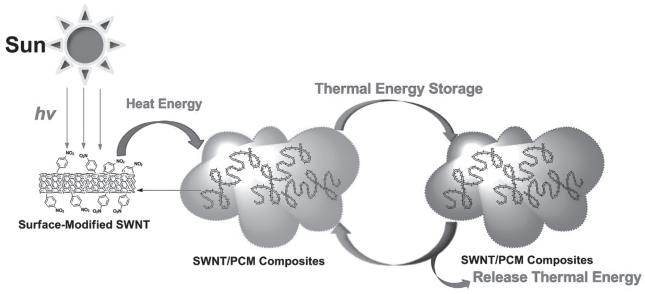

Figure 1. Schematic diagram of light-to-heat conversion and storage.

Due to large π–π interactions between the PCMs and the surface-modified SWNTs, the SWNTs were effectively dispersed and stabilized in toluene.[14] Then, the SWNT/PCM composite preparations were performed using simple physical methods of vacuum-evaporation and further drying for 48 h at 80 °C under vacuum (–0.1 kPa) prior to testing. MWNT/PCM and CB/PCM composites were obtained according to the above-described procedures. The resulting composites are abbreviated throughout the manuscript as listed in **Table 1**.

Table 1. Sample identification and composition.

Sample	Composition
PEG 10000	PEG 10000
PCM	PEG 10000:TDI:*N*,*N*'-dihydroxyethyl aniline = 1:2:1[a)]
SWNT/PCM-1	surface-modified SWNT:PCM = 0.5:100[b)]
SWNT/PCM-2	surface-modified SWNT:PCM = 1:100
SWNT/PCM-3	surface-modified SWNT:PCM = 2:100
SWNT/PCM-4	surface-modified SWNT:PCM = 3:100
SWNT/PCM-5	surface-modified SWNT:PCM = 4:100
MWNT/PCM	surface-modified MWNT:PCM = 2:100
Carbon black (CB)/PCM	surface-modified CB:PCM = 2:100

[a)]Molar ratios of polyethylene glycol (PEG), toluene-2,4-diisocyanate (TDI), and *N*,*N*-dihydroxyethyl aniline; [b)]Mass ratios of surface-modified SWNTs and PCMs.

2.1. Sunlight Irradiation

The UV-vis-NIR spectrum of the synthesized composite, showed in **Figure 2**a, demonstrated absorption over a wide range of the spectrum. The SWNTs in the SWNT/PCM composites exhibit one total absorbance characteristic in the UV-vis-NIR region as a result of van Hove transitions,[15] which are very important for the effective light harvesting of solar irradiation. Figure 2b shows the incident photon-to-thermal conversion spectra of the SWNT/PCM composites. The detailed experiments are described in the Supporting Information. Compared with the pure PEG 10000 (black line in Figure 2b), the temperature of the SWNT/PCM composites rapidly increased (colored line in Figure 2b) upon solar irradiation. This behavior is ascribed to the function of SWNTs as an effective photon captor and molecular heater. SWNTs display optical absorptions due to resonant band-to-band transitions[15c] and π-plasmon excitation.[16] Simultaneously, the temperature of the control sample (PEG 10000) also gradually increased because the PEG absorbed the near-infrared light of the solar irradiation.[17] The temperature growth platform of the SWNT/PCM composites appeared between 49.3 and 58.1 °C as the irradiation time increased. This phenomenon illustrates that the phase transition of the SWNT/PCM composites has occurred upon solar irradiation, when the SWNT/PCM composites absorbed solar radiation, converted the radiation into thermal energy and stored the resulting energy in PCMs. As shown in Figure 2b, the temperature of the SWNT/PCM composites rapidly decreased after covering the solar irradiation. The composites then exhibited cool temperature platforms. Thus, a larger amount of heat energy was released by the SWNT/PCM composites in the form-stable phase change process. This result showed that the SWNTs functioned as an effective photon captor and device heater by converting light into heat energy. The heat energy was stored in the SWNT/PCM composites through the phase transition.

To improve the sunlight-harvesting and light-thermal conversion efficiency further, we changed the SWNT quantity as a photon captor and device heater for the thermal phase transition of the phase change materials. As shown in Figure 2b, when the SWNT content of SWNT/PCM composites was increased, the temperatures of SWNT/PCM-2 to -5 increased faster and the platform of the temperatures was significantly shorter than SWNT/PCM-1 upon solar irradiation. However, only a slight change occurred in the phase transition enthalpy and temperature (**Figure 3** and **Table 2**).

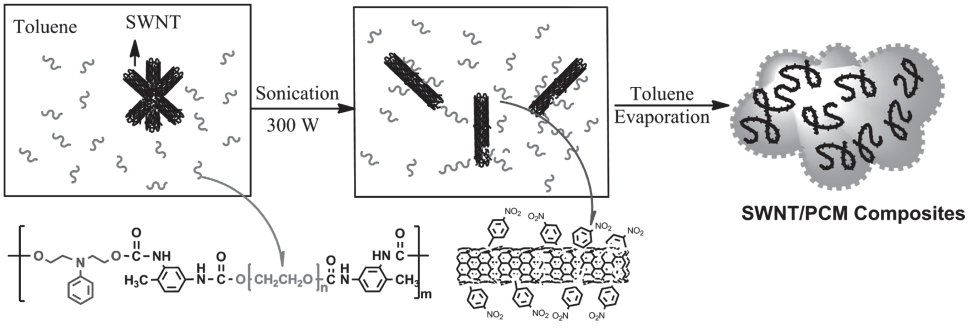

Scheme 1. The hybridization process of SWNT/PCM composites.

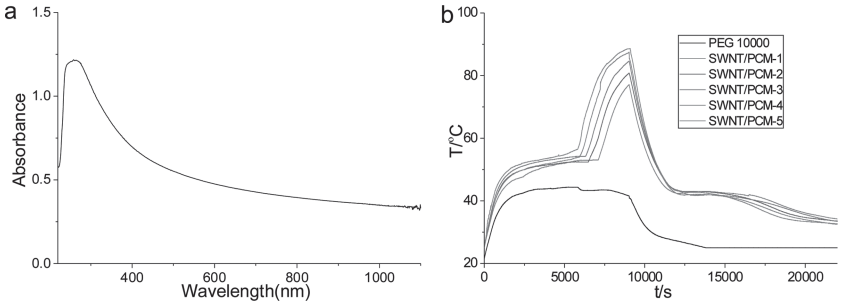

Figure 2. a) UV-vis-NIR absorption spectrum of the surface-modified SWNTs in toluene. b) Light-thermal conversion curves of the samples under sunlight radiation (P = 0.25–0.26 W, ambient temperature = 24.3 °C, 11:57–13:13, September 18, 2012, Dalian, China).

Of critical importance is the light-to-heat and energy storage efficiency (η) of the SWNT/PCM composites. Using photothermal calculation methods, the obtained η of SWNT/PCM 1 to 5, MWNT/PCM and CB/PCM composites was 0.845, 0.857, 0.872, 0.885, 0.913, 0.848 and 0.826, respectively. The value of η was calculated according to Equation (2) and Supporting Information Figure S1, as expected for solar energy materials.

2.2. Thermal Properties

Figure 3 shows the differential scanning calorimetry (DSC) curves of the pure PEG 10000, PCM, SWNT/PCM, MWNT/PCM, and CB/PCM composites. The thermal energy storage data obtained from the DSC curves are also listed in Table 2. Compared with the pure PEG (197.2 J/g), the PCM (about 100 J/g) exhibited a partial loss in latent heat (Figure 3 and Table 2). This result is due to the restriction of pure PEG crystallisation in the PCM caused by the solid portion of *N,N*-dihydroxyethyl aniline. It is important for the SWNT/PCM composites to remain form-stable during the entire heating process. The DSC curves of the PCM and SWNT/PCM composites in Figure 3 are virtually identical to those listed in Table 2. In addition, the negligible effect of the SWNT/PCM composites affected the phase transition temperature and enthalpy. Moreover, the SWNT/PCM composites exhibited high energy storage densities, all of which exceeded 100 J/g. In other words, these thermal energy of SWNT/PCM composites obtained by phase transition can heat an equivalent quantity of PEG 10000 to elevated temperatures of 50 °C.

Thermal conductivity is of vital importance to solar thermal energy storage materials. SWNT/PCM composites with high thermal conductivity can shorten the time of heat storage and release, which improves the energy utilization efficiency. The thermal conductivities of PCM, SWNT/PCM-3, MWNT/PCM and CB/PCM composites are 0.267, 0.334, 0.312, and 0.280 W/(mK), respectively. Compared with PCM, the thermal conductivities of SWNT/PCM-3, MWNT/PCM and CB/PCM composites were enhanced by 25.1%, 16.9% and 4.9%, respectively. Although the η and the phase transition temperature and enthalpy of these carbon/PCM composites were similar with each others, the thermal conductivity of SWNT/PCM-3 composite was obviously improved as compared to other carbon/PCM composites (MWNT/PCM and CB/PCM). Additionally, the enhancement of the thermal transfer rate was also investigated by comparing the heating and freezing processes (Supporting Information Figure S2). The results demonstrated that to achieve the same temperature of 60 °C, the required heating time of SWNT/PCM-3, MWNT/PCM and CB/PCM composites was 870, 970, and 1065 s during the heating process (Supporting Information Figure S2a), respectively. Obviously, the heating time of the form-stable SWNT/PCM-3 composite was reduced by 10.3% and 18.3% as compared to that of MWNT/PCM and CB/PCM composites, respectively. As for the freezing process (Supporting Information Figure S2b), to achieve the same temperature of 40 °C, the freezing time of SWNT/PCM-3, MWNT/PCM and CB/PCM composites was 940 s, 1075 s and 1195 s, respectively. The freezing time of the form-stable SWNT/PCM-3 composite was reduced by 12.6% and 21.3% as compared to that of MWNT/PCM and CB/PCM composites, respectively. Therefore, compared with other carbon/PCM composites (MWNT/PCM or CB/PCM), our composites have a highly thermal conductivity, which improves

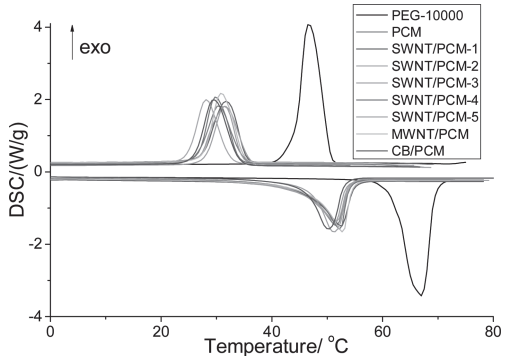

Figure 3. DSC curves of PEG 10000, PCM, SWNT/PCM, MWNT/PCM and CB/PCM composites.

Table 2. Phase-change behavior of PEG 10000, PCM, and SWNT/PCM, MWNT/PCM and CB/PCM composites.

Sample	Phase transition	ΔH [J/g]		T_r [°C]	
		Heating cycle	Cooling cycle	Heating cycle	Cooling cycle
PEG 10000	Solid–liquid	197.2	201.1	67.0	46.7
PCM	Form–stable	100.3	100.2	51.7	30.4
SWNT/PCM-1	Form–stable	103.2	103.4	52.5	31.7
SWNT/PCM-2	Form–stable	101.5	101.1	51.5	28.1
SWNT/PCM-3	Form–stable	100.5	100.3	51.6	31.5
SWNT/PCM-4	Form–stable	100.4	99.8	52.3	29.9
SWNT/PCM-5	Form–stable	98.1	90.1	51.9	31.4
MWNT/PCM	Form–stable	100.0	101.3	52.7	30.4
CB/PCM	Form–stable	100.6	101.4	51.1	29.3

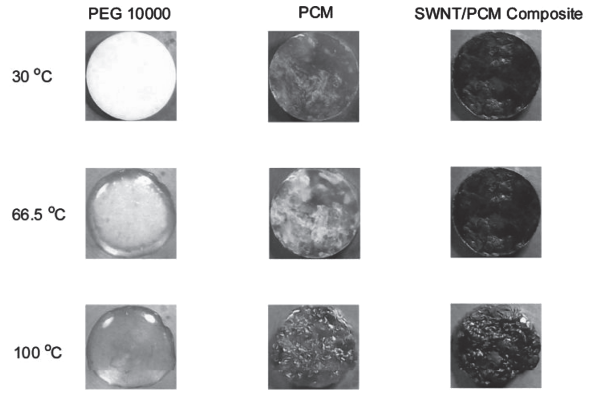

Figure 4. Form-stable effect for the PEG 10000, PCM, and SWNT/PCM composites with increasing temperature.

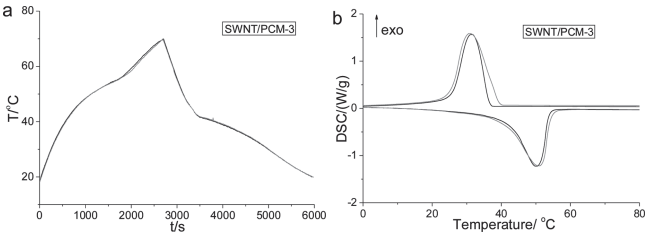

Figure 5. a) Simulated sunlight irradiation spectra of the SWNT/PCM composites before (black line) and after (red line) 100 cycles of light irradiation (P = 1.10 W, m = 5.0 g, light irradiation, ambient temperature = 16.4 °C). b) DSC curves of the SWNT/PCM composites before (black line) and after (red line) the 100 cycles of irradiation.

the energy utilisation efficiency during heat charging and discharging processes.

2.3. Form-Stable Properties

The form-stable properties are crucial aspects of organic phase change materials. The shape-stabilized properties of the pure PEG, PCM, and SWNT/PCM composites were characterized using hot stage-digital camera technology. The samples were placed briefly on a hot stage and then heated from 30 to 100 °C at a rate of 5 °C/min. The changes in the samples were observed via tracking photography using a digital camera. Although the pure PEG and the SWNT/PCM composites both underwent phase transitions with high-transition enthalpies, their phase-transition states significantly differed. The PCM and SWNT/PCM composites remained solid unlike the pure PEG 10000, which exhibited a solid-to-liquid phase transition (**Figure 4**). In addition, no liquid was observed during the entire heating process, even when the temperature exceeded 100 °C. Thus, the SWNT/PCM composites exhibited a large energy-storage effect and shape-stabilized property, thereby extending their application in other fields. A preliminary study showed that SWNT/PCM composites exhibited high strength and flexibility (Supporting Information Figure S3,S4). Therefore, SWNT/PCM composites may be used as smart clothing or leather through fabric blending or wire drawing. Additionally, due to the performance of strong near-infrared absorbance characteristic and high heat storage density with minor temperature change during form-stable phase change processes, the SWNT/PCM composites have a potential application in military infrared stealth.

2.4. Reversible Stability

To prove the photodriven phase change reversibility of the SWNT/PCM composites, simulated sunlight irradiation cycling tests were performed, and the results of a 100 cycle test are shown in **Figure 5**. The tests were conducted during simulated light irradiation for 20 min, followed by the irradiation being covered for 20 min in a temperature-controlled water bath (10 °C) to ensure the solid-solid cycles. The spectral features of the first cycle (black line in Figure 5a) and the 100th cycle irradiation (red line in Figure 5a) were virtually identical. Additionally, the SWNT/PCM composites were then checked with DSC for their latent heat storage capacity (Figure 5b). Compared with 100.5 and 100.3 J/g before the cycles, the latent heats of melting and freezing were 100.7 and 100.9 J/g after 100 cycles, respectively. Amazingly, the excellent reversibility of the SWNT/PCM composites was observed, even after operating for 100 cycles.

2.5. XRD Analysis

The XRD patterns of the pure PEG, PCM, and SWNT/PCM composites are shown in **Figure 6** to furhter reveal the crystallization patrerns. Sharp and intense diffraction peaks at 19.12° and 23.24° were observed in the PCM and SWNT/PCM composites. These values are similar to the characteristic peaks of PEG.[6c] The PCM and SWNT/PCM composites showed diffraction curves similar to those of pure PEG. The diffraction angle and the crystal plane distance were nearly the same. These results indicate that the PCM and SWNT/PCM composites still have good crystalline properties. These properties are consistent with the previously discussed DSC results.

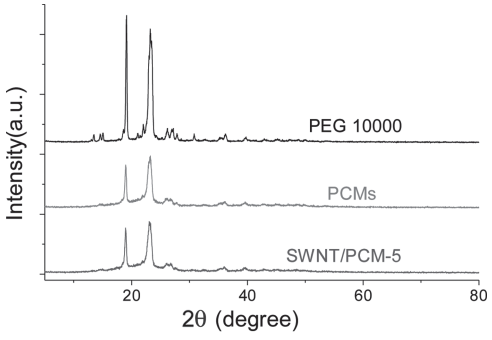

Figure 6. XRD patterns of the PEG 10000, PCMs, and SWNT/PCM composites.

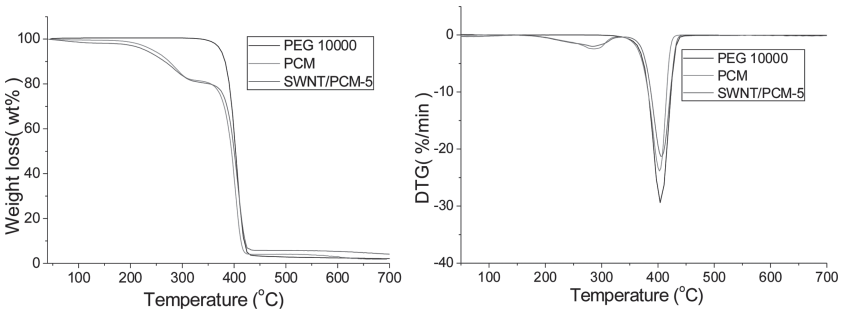

Figure 7. TG and DTG curves of the PEG 10000, PCM, and SWNT/PCM composites.

Table 3. Thermal stability properties of the PEG 10000, PCM, and SWNT/PCM composites.

Sample	T_{max1} [°C]	T_{max2} [°C]	Char yield at 700 °C [wt%]
PEG 10000	/	403.9	2.1
PCM	286.4	402.7	1.8
SWNT/PCM-5	284.1	406.2	4.1

2.6. Thermal Stability

Thermal stability is vital to pure organic compounds. In this study, thermogravimetric (TG) and derivative TG (DTG) analyses were conducted to determine the thermal stability of the SWNT/PCM composites. The corresponding results are presented in **Figure 7** and **Table 3**. The PCM and SWNT/PCM composites underwent a two-step degradation process. The first step involved the degradation of the PCM and SWNT/PCM polyurethane chain between 284 and 287 °C.[18] The second step occurred at approximately 400 to 410 °C. This step corresponds to the degradation of the pure PEG chain.[19] The actual weight losses of the PCM and SWNT/PCM composites are nearly equal to the theoretical amount during the first degradation step. Table 3 lists the charred SWNT/PCM composite residue percentages. These values are identical to the charred PEG residue percentages at 700 °C and are close to the theoretical results for organic compounds. Therefore, the TGA results are consistent with the expected degradation mechanism. The results also show that the SWNT/PCM composite exhibits high thermal stabilities. Thus, the requirements for practical application are met.

3. Conclusions

Novel SWNT/PCM composites were designed and synthesized. The resulting SWNT/PCM composites demonstrated several unique characteristics, such as a wider absorption range for sunlight, high light-to-heat conversion and energy storage efficiencies, as well as excellent form-stable properties. The simplicity of these composites provides a new platform for improving the solar radiation usage efficiency, which can be widely applied to fields related to energy conversion and storage. Simultaneously, a preliminary study showed that SWNT/PCM composites may be used as smart clothing or leather through fabric blending or wire drawing. Additionally, our composites exhibited strong near-infrared absorbance characteristics and high energy storage density with minor temperature change during heat storage and release processes, which have a potential application in military stealth.

4. Experimental Section

Materials: The SWNTs with less than 2 nm diameter and 5–10 um length (special surface area: 350–400 m^2/g, purity: 90%) used in this research were purchased from Shenzhen Nanotech Prot Co., Ltd. MWNTs with 8–15 nm diameter and 0.5–2 um length (special surface area: >233 m^2/g, purity: >95%) were purchased from China Sciences Academy Chengdu Organic Chemical Co., Ltd. Carbon black (CB) M900 was purchased from Cabot Corp. Analytical grade polyethylene glycol (PEG, M_n = 10 000, Shanghai National Medicines Co. Inc., China) was dried at 80 °C under high vacuum (–0.1 kPa) for 48 h. Analytical grade toluene (Tianjin National Medicines Co. Inc., China) was dried for 48 h by using a 5 Å molecular sieve and then distilled prior to use. Analytical grade toluene-2,4-diisocyanate (TDI, Tianjin Kemiou Chemical Reagent Co. Inc., China) and dibutyltin dilaurate (DBT, Tianjin Kemiou Chemical Reagent Co. Inc., China) were used as received. All other reagents were of analytical grade.

Synthesis of the Form-Stable PCM: The synthetic route for preparing the PCM is shown in **Scheme 2**. The synthesis was conducted in a flame-dried glassware through a two-step polymerisation process in an inert nitrogen (N_2) atmosphere. First, a predetermined amount of

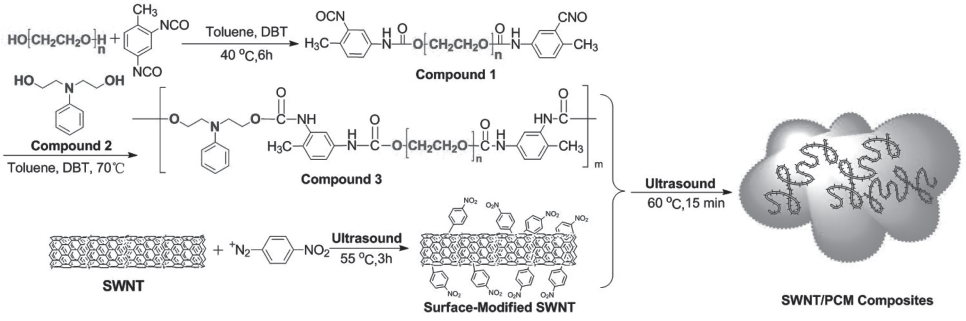

Scheme 2. Chemical structures and synthetic scheme for the SWNT/PCM composites.

dried PEG 10000, TDI, and DBT was mixed in freshly distilled toluene and stirred for 6 h in an N_2 atmosphere at 40 to 45 °C to produce an NCO-terminated prepolymer (Compound 1). A stoichiometric amount of the chain extender (Compound 2) was added, and the reactions were continued for 6 h at 100 °C. The molecular weights of PEG 10000-CO-*N*,*N*-dihydroxyethyl aniline were evaluated from the intrinsic viscosity (η) measured in the toluene solvent using an Ubbelohde capillary viscometer at 25 °C. According to a previous report,[20] the viscosity-average molecular weight (M_v) of the obtained PCM was related to the intrinsic viscosity based on Equation (1):

$$|\eta| = 2.1 \times 10^{-4} \times \bar{M}_v^{0.82} \quad (1)$$

where M_v of the obtained form-stable PCM found to be approximately 1.92×10^7 using Equation (1).

Synthesis of the Surface-Modified SWNTs: The SWNTs were modified according to a method published in the literature,[21] which involved grafting 4-nitrophenyl moieties onto the surface of the SWNT substrates. The synthetic process for preparing surface-modified SWNTs is shown in Scheme 2. The in situ-generated diazonium cation modification was conducted by dispersing 1.0 g of SWNTs in 50 mL of deionized water, to which 10 mmol 4-nitroaniline was added, followed by 10 mmol sodium nitrite, and finally 12 mL of concentrated hydrochloric acid. The mixture was ultrasonicated at 300 W for 3 h at 55 °C, and stirred overnight at ambient temperature, filtered, and then washed successively with water and methanol. The resulting SWNTs were dried overnight under vacuum, and the product was labelled as surface-modified SWNTs.

Synthesis of the SWNT/PCM Composites: A specific amount of the surface-modified SWNTs and a known concentration of the reaction liquid obtained above were mixed and thoroughly stirred (Scheme 2). The mixture was ultrasonicated at 300 W for 15 min at 60 °C to obtain a well-dispersed suspension. The solution containing the resulting SWNT/PCM composite was vacuum-evaporated and then further dried for 48 h at 80 °C under vacuum (–0.1 kPa) prior to testing, producing the final SWNT/PCM composites.

Other carbon/PCM composites (MWNT/PCM and CB/PCM composites) were obtained according to the above-described procedures.

Transduction and Storage Efficiency of the SWNT/PCM Composites: The visible light-to-heat transduction and energy storage efficiency (η) of the SWNT/PCM composites was calculated using Equation (2) through irradiation from a simulated light source (with a measured light irradiation area of 4.90 cm^2).[22] The temperature of the SWNT/PCM composites was measured within foam insulation after simulating the light source irradiation (UV-vis light). When photothermal calculation methods were used, the parameter η was obtained as follows:

$$\eta = \frac{m\Delta H}{P(t_t - t_f)} \quad (2)$$

where η is the light-to-heat conversion and thermal storage efficiency, m is the quality of the SWNT/PCM composites, ΔH is the transition enthalpy of the SWNT/PCM composites obtained by conducting differential scanning calorimetry (DSC), t_t and t_f are the light-driven phase transition time of the SWNT/PCM composites before and after the phase change, respectively, and P is the power for the light irradiation of the simulated light source.

Characterization: The physical and chemical characterization of the SWNT/PCM composites, SWNT, PEG 10000, and PCM were performed as described in the following paragraphs.

The structural analysis of the SWNT/PCM composites and the SWNTs was performed using a Fourier transform infrared spectrophotometer (Nicolet Avatar 320, KBr pellets). A proton nuclear magnetic resonance analysis (in DMSO-d_6, with TMS as the internal standard) was performed on a Bruker AV-400 spectrometer. The chemical shifts were reported in ppm.

The structural characterization of the SWNT/PCM composites and PCMs is reported in the Supporting Information.

The methods for the sunlight irradiation experiments and the transduction and storage efficiency were reported in our previous study.[22]

DSC was performed in an N_2 atmosphere using a 910S DSC thermal analyser (TA Instruments, America) from 0 to 80 °C at a heating rate of 5 °C/min, an N_2 flow rate of 20 mL/min, a calorimeter precision of ±2.0%, and temperature measurements of ±2.0 °C. The samples were measured in a sealed aluminium pan with a mass of approximately 5.0 mg. The latent heat was calculated as the total area under the transition peaks of the SWNT/PCM composites using thermal analysis software.

The shape-stabilized properties of the SWNT/PCM composites were characterized using hot stage-digital camera technology. The samples were placed on a hot stage and heated from 30 to 100 °C at a rate of 5 °C/min. The changes in the samples were observed via tracking photography by using a digital camera.

The thermal stability properties were characterized via thermogravimetric analysis (TGA) by using a TGA/SDTA 851 thermal analyser (Mettler-Toledo, Switzerland). Approximately 10 mg of the specimen was heated from 40 to 700 °C at a linear heating rate of 10 °C/min in an N_2 atmosphere.

X-ray diffraction (XRD) experiments were directly performed on the samples at room temperature using a D/Max2400 (Rigaku, Japan) in the 5° to 80° range.

The thermal conductivities were measured using a DRL-III tester (Xiangyi Instrument, China).

Supporting Information

Supporting Information is available from the Wiley Online Library or from the author.

Acknowledgements

This work was supported by the National Natural Science Foundation of China (21276042), the National Science and Technology Pillar Program (2013BAF08B06), and the Jiaogai Foundation of DUT (JGXM201224).

Received: December 17, 2012
Revised: February 6, 2013
Published online: May 10, 2013

[1] a) N. Robertson, *Angew. Chem. Int. Ed.* **2008**, *47*, 1012; b) V. Cristino, S. Caramori, R. Argazzi, L. Meda, G. L. Marra, C. A. Bignozzi, *Langmuir* **2010**, *27*, 7276; c) D. Kraemer, B. Poudel, H.-P. Feng, J. C. Caylor, B. Yu, X. Yan, Y. Ma, X. Wang, D. Wang, A. Muto, K. McEnaney, M. Chiesa, Z. Ren, G. Chen, *Nat. Mater.* **2011**, *10*, 532; d) W. Ying, F. Guo, J. Li, Q. Zhang, W. Wu, H. Tian, J. Hua, *ACS Appl. Mater. Interfaces* **2012**, *4*, 4215; e) F. Hao, X. Wang, C. Zhou, X. Jiao, X. Li, J. Li, H. Lin, *J. Phys. Chem. C* **2012**, *116*, 19164–19172; f) L. Dai, *Acc. Chem. Res.* **2012**, *46*, 31; g) X. Shengqiang, C. P. Samuel, Z. Huaxing, Y. Wei, *Functional Polymer Nanocomposites for Energy Storage and Conversion, Vol. 1034,* American Chemical Society, Washington **2010**, pp. 71–80; h) K. W. J. Barnham, M. Mazzer, B. Clive, *Nat. Mater.* **2006**, *5*, 161; i) C. Liu, F. Li, L.-P. Ma, H.-M. Cheng, *Adv. Mater.* **2010**, *22*, E28; j) T. M. Tritt, H. Böttner, L. Chen, *MRS Bull.* **2008**, *33*, 366; k) N. Armaroli, V. Balzani, *Angew. Chem. Int. Ed.* **2007**, *46*, 52.

[2] C. G. Granqvist, *Adv. Mater.* **2003**, *15*, 1789.

[3] a) Z. Han, A. Fina, *Prog. Polym. Sci.* **2011**, *36*, 914; b) N. Nuraje, X. Dang, J. Qi, M. A. Allen, Y. Lei, A. M. Belcher, *Adv. Mater.* **2012**, *24*, 2885.
[4] a) N. W. S. Kam, M. O'Connell, J. A. Wisdom, H. Dai, *Proc. Natl. Acad. Sci. USA* **2005**, *102*, 11600; b) T. Fujigaya, T. Morimoto, Y. Niidome, N. Nakashima, *Adv. Mater.* **2008**, *20*, 3610.
[5] a) D. Yu, K. Park, M. Durstock, L. Dai, *J. Phys. Chem. Lett.* **2010**, *2*, 1113; b) K. Vandewal, K. Tvingstedt, A. Gadisa, O. Inganas, J. V. Manca, *Nat. Mater.* **2009**, *8*, 904.
[6] a) E. Miyako, H. Nagata, K. Hirano, T. Hirotsu, *Angew. Chem. Int. Ed.* **2008**, *47*, 3610; b) P. M. Ajayan, M. Terrones, A. de la Guardia, V. Huc, N. Grobert, B. Q. Wei, H. Lezec, G. Ramanath, T. W. Ebbesen, *Science* **2002**, *296*, 705; c) M. Eijiro, N. Hideya, H. Ken, M. Yoji, N. Ken-ichi, H. Takahiro, *Nanotechnology* **2007**, *18*, 475103; d) M. Eijiro, N. Hideya, H. Ken, S. Kotaro, M. Yoji, N. Ken-ichi, H. Takahiro, *Nanotechnology* **2008**, *19*, 075106.
[7] a) A. A. Aljaafari, S. S. Ibrahim, T. A. El-Brolossy, *Composites, Part A* **2011**, *42*, 394; b) S. Harish, K. Ishikawa, E. Einarsson, S. Aikawa, S. Chiashi, J. Shiomi, S. Maruyama, *Int. J. Heat Mass Transfer* **2012**, *55*, 3885.
[8] Y. Shen, A. G. Skirtach, T. Seki, S. Yagai, H. Li, H. Möhwald, T. Nakanishi, *J. Am. Chem. Soc.* **2010**, *132*, 8566.
[9] a) K. A. R. Ismail, F. A. M. Lino, *Exp. Therm. Fluid Sci.* **2011**, *35*, 1010; b) F. Agyenim, N. Hewitt, P. Eames, M. Smyth, *Renewable Sustainable Energy Rev.* **2010**, *14*, 615; c) A. Koca, H. F. Oztop, T. Koyun, Y. Varol, *Renewable Energy* **2008**, *33*, 567.
[10] J. T. McCann, M. Marquez, Y. Xia, *Nano Lett.* **2006**, *6*, 2868.
[11] A. Thess, R. Lee, P. Nikolaev, H. Dai, P. Petit, J. Robert, C. Xu, Y. H. Lee, S. G. Kim, A. G. Rinzler, D. T. Colbert, G. E. Scuseria, D. Tománek, J. E. Fischer, R. E. Smalley, *Science* **1996**, *273*, 483.
[12] O.-K. Kim, J. Je, J. W. Baldwin, S. Kooi, P. E. Pehrsson, L. J. Buckley, *J. Am. Chem. Soc.* **2003**, *125*, 4426.
[13] a) M. F. Islam, E. Rojas, D. M. Bergey, A. T. Johnson, A. G. Yodh, *Nano Lett.* **2003**, *3*, 269; b) Y. Kang, T. A. Taton, *J. Am. Chem. Soc.* **2003**, *125*, 5650; c) N. Stürzl, F. Hennrich, S. Lebedkin, M. M. Kappes, *J. Phys. Chem. C* **2009**, *113*, 14628; d) T. Liu, S. Luo, Z. Xiao, C. Zhang, B. Wang, *J. Phys. Chem. C* **2008**, *112*, 19193.
[14] a) C. Schulz-Drost, V. Sgobba, C. Gerhards, S. Leubner, R. M. Krick Calderon, A. Ruland, D. M. Guldi, *Angew. Chem. Int. Ed.* **2010**, *49*, 6425; b) J. Zhu, B. S. Shim, M. Di Prima, N. A. Kotov, *J. Am. Chem. Soc.* **2011**, *133*, 7450; c) Q. Bao, H. Zhang, J.-x. Yang, S. Wang, D. Y. Tang, R. Jose, S. Ramakrishna, C. T. Lim, K. P. Loh, *Adv. Funct. Mater.* **2010**, *20*, 782.
[15] a) M. J. O'Connell, S. M. Bachilo, C. B. Huffman, V. C. Moore, M. S. Strano, E. H. Haroz, K. L. Rialon, P. J. Boul, W. H. Noon, C. Kittrell, J. Ma, R. H. Hauge, R. B. Weisman, R. E. Smalley, *Science* **2002**, *297*, 593; b) P. J. Boul, J. Liu, E. T. Mickelson, C. B. Huffman, L. M. Ericson, I. W. Chiang, K. A. Smith, D. T. Colbert, R. H. Hauge, J. L. Margrave, R. E. Smalley, *Chem. Phys. Lett.* **1999**, *310*, 367; c) S. M. Bachilo, M. S. Strano, C. Kittrell, R. H. Hauge, R. E. Smalley, R. B. Weisman, *Science* **2002**, *298*, 2361.
[16] a) B. W. Reed, M. Sarikaya, *Phys. Rev. B* **2001**, *64*, 195404; b) B. W. Reed, M. Sarikaya, L. R. Dalton, G. F. Bertsch, *Appl. Phys. Lett.* **2001**, *78*, 3358; c) S. Attal, R. Thiruvengadathan, O. Regev, *Anal. Chem.* **2006**, *78*, 8098.
[17] N. Sarier, E. Onder, *Thermochim. Acta* **2007**, *454*, 90.
[18] a) M. A. Izquierdo, F. J. Navarro, F. J. Martínez-Boza, C. Gallegos, *Constr. Build. Mater.* **2012**, *30*, 706; b) Q. Cao, P. S. Liu, *Eur. Polym. J.* **2006**, *42*, 2931.
[19] Q. H. Meng, J. L. Hu, *Sol. Energy Mater. Sol. Cells* **2008**, *92*, 1245.
[20] H. Lu, H. Wang, A. Zheng, H. Xiao, *Polym. Compos.* **2007**, *28*, 42.
[21] M. Toupin, D. Belanger, *Langmuir* **2008**, *24*, 1910.
[22] Y. Wang, B. Tang, S. Zhang, *J. Mater. Chem.* **2012**, *22*, 18145.